Cubic spline wavelets with short support for fourth-order problems

Dana Černá[a], Václav Finěk[a]

[a]*Department of Mathematics and Didactics of Mathematics, Technical University in Liberec, Studentská 2, 461 17 Liberec, Czech Republic*

Abstract

In the paper, we propose a construction of new cubic spline-wavelet bases on the unit cube satisfying homogeneous Dirichlet boundary conditions of the second order. The basis functions have small supports and wavelets have vanishing moments. We show that stiffness matrices arising from discretization of the biharmonic problem using a constructed wavelet basis have uniformly bounded condition numbers and these condition numbers are very small. We present quantitative properties of the constructed bases and we show a superiority of our construction in comparison to some other cubic spline wavelet bases satisfying boundary conditions of the same type.

Keywords: wavelet, cubic spline, homogeneous Dirichlet boundary conditions, condition number, biharmonic problem
2000 MSC: 46B15, 65N12, 65T60

1. Introduction

In recent years wavelets have been successfully used for solving various types of differential equations [8, 9] as well as integral equations [17, 19, 20]. The quantitative properties of wavelet methods strongly depend on the choice of a wavelet basis, in particular on its condition number. Therefore, a construction of a wavelet basis is an important issue.

In this paper, we propose a construction of cubic spline wavelet bases on the interval that are well-conditioned, adapted to homogeneous Dirichlet

Email addresses: dana.cerna@tul.cz (Dana Černá), vaclav.finek@tul.cz (Václav Finěk)

Preprint submitted to Applied Mathematics and Computation

boundary conditions of the second order, the wavelets have vanishing moments and the shortest possible support. The wavelet basis of the space $H_0^2\left((0,1)^2\right)$ is then obtained by an isotropic tensor product. We compare the condition numbers of the corresponding stiffness matrices for various constructions. Finally, a quantitative behaviour of an adaptive wavelet method for several boundary-adapted cubic spline wavelet bases is studied.

First of all, we summarize the desired properties of a constructed basis:

- *Riesz basis property.* We construct Riesz bases of the space $H_0^2(0,1)$ and $H_0^2\left((0,1)^2\right)$.
- *Polymial exactness.* Since the primal basis functions are cubic B-splines, the primal multiresolution analysis has polynomial exactness of order four.
- *Vanishing moments.* The inner wavelets have two vanishing moments, the wavelets near the boundary can have less vanishing moments.
- *Short support.* The wavelets have the shortest possible support for a given number of vanishing moments.
- *Locality.* The primal basis functions are local.
- *Closed form.* The primal scaling functions and wavelets are known in the closed form.
- *Homogeneous Dirichlet boundary conditions.* Our wavelet bases satisfy homogeneous Dirichlet boundary conditions of the second order.
- *Well-conditioned bases.* Our objective is to construct a well conditioned wavelet basis.

Moreover, in a comparison with constructions in [1, 4, 11, 21, 22] that are quite long and technical, the construction in this paper is very simple. Many constructions of cubic spline wavelet or multiwavelet bases on the interval have been proposed in recent years. In [2, 4, 11, 21] cubic spline wavelets on the interval were constructed. In [10] cubic spline multiwavelet bases were designed and they were adapted to complementary boundary conditions of the second order in [22]. In these cases dual functions are known and are local. Cubic spline wavelet or multiwavelet bases where duals are not local were constructed in [7, 14, 15, 16]. Some of these bases were already adapted to boundary conditions and used for solving differential equations [6, 18]. The advantage of our construction is the shortest possible support for a given number of required vanishing moments. Vanishing moments are necessary in some applications such as adaptive wavelet methods [8, 9]. Originally, these methods were designed for wavelet bases with local duals. However, it was shown in [12] that wavelet bases without local dual basis can be used if the solved equation is linear.

This paper is organized as follows: In Section 2 we briefly review the concept of wavelet bases. In Section 3 we propose a construction of primal and dual scaling bases. The refinement matrices are computed in Section 4. In Section 5 the properties of the projectors associated with constructed bases are derived and the proof that the bases are indeed Riesz bases is given. Quantitative properties of constructed bases and other known cubic spline wavelet and multiwavelet bases are studied in Section 6. In Section 7 we compare the number of basis functions and the number of iterations needed to resolve the problem with desired accuracy for bases constructed in this paper and bases from [4, 22]. A numerical example is presented for an equation with the biharmonic operator in two dimensions.

2. Wavelet bases

This section provides a short introduction to the concept of wavelet bases in Sobolev spaces. In this paper, we consider the domain $\Omega = (0,1)$ or $\Omega = (0,1)^2$. We denote the Sobolev space or its subspace by $H \subset H^s(\Omega)$ for nonnegative integer s and the corresponding inner product by $\langle \cdot, \cdot \rangle_H$, a norm by $\|\cdot\|_H$ and a seminorm by $|\cdot|_H$. In case $s = 0$ we consider the space $L^2(\Omega)$ and we denote by $\langle \cdot, \cdot \rangle$ and $\|\cdot\|$ the L^2-inner product and the L^2-norm, respectively. Let $\mathcal{J}$ be some index set and let each index $\lambda \in \mathcal{J}$ take the form $\lambda = (j, k)$, where $|\lambda| := j \in \mathbb{Z}$ is a *scale* or a *level*. Let

$$\|\mathbf{v}\|_{l^2(\mathcal{J})} := \sqrt{\sum_{\lambda \in \mathcal{J}} |v_\lambda|^2}, \text{ for } \mathbf{v} = \{v_\lambda\}_{\lambda \in \mathcal{J}}, \, v_\lambda \in \mathbb{R}, \tag{1}$$

and

$$l^2(\mathcal{J}) := \left\{ \mathbf{v} : \mathbf{v} = \{v_\lambda\}_{\lambda \in \mathcal{J}}, \, v_\lambda \in \mathbb{R}, \|\mathbf{v}\|_{l^2(\mathcal{J})} < \infty \right\}. \tag{2}$$

A family $\Psi := \{\psi_\lambda, \lambda \in \mathcal{J}\}$ is called a *(primal) wavelet basis* of H, if

i) Ψ is a *Riesz basis* for H, i.e. the closure of the span of Ψ is H and there exist constants $c, C \in (0, \infty)$ such that

$$c \|\mathbf{b}\|_{l^2(\mathcal{J})} \leq \left\| \sum_{\lambda \in \mathcal{J}} b_\lambda \psi_\lambda \right\|_H \leq C \|\mathbf{b}\|_{l^2(\mathcal{J})}, \quad \mathbf{b} := \{b_\lambda\}_{\lambda \in \mathcal{J}} \in l^2(\mathcal{J}). \tag{3}$$

Constants $c_\psi := \sup\{c : c \text{ satisfies } (3)\}$, $C_\psi := \inf\{C : C \text{ satisfies } (3)\}$ are called *Riesz bounds* and *cond* $\Psi = C_\psi / c_\psi$ is called the *condition number* of Ψ.

ii) The functions are *local* in the sense that $\operatorname{diam}(\Omega_\lambda) \leq C2^{-|\lambda|}$ for all $\lambda \in \mathcal{J}$, where Ω_λ is the support of ψ_λ, and at a given level j the supports of only finitely many wavelets overlap at any point $x \in \Omega$.

By the Riesz representation theorem, there exists a unique family $\tilde{\Psi} = \left\{\tilde{\psi}_\lambda, \lambda \in \tilde{\mathcal{J}}\right\} \subset H$ biorthogonal to Ψ, i.e.

$$\left\langle \psi_{i,k}, \tilde{\psi}_{j,l} \right\rangle_H = \delta_{i,j}\delta_{k,l}, \quad \text{for all} \quad (i,k) \in \mathcal{J}, \quad (j,l) \in \tilde{\mathcal{J}}, \tag{4}$$

where $\delta_{i,j}$ denotes the Kronecker delta, i.e. $\delta_{i,j} = 1$ for $i = j$ and $\delta_{i,j} = 0$ for $i \neq j$. This family is also a Riesz basis for H, but the functions $\tilde{\psi}_{j,l}$ need not be local. The basis $\tilde{\Psi}$ is called a *dual* wavelet basis.

In many cases, the wavelet system Ψ is constructed with the aid of a multiresolution analysis. A sequence $\mathcal{V} = \{V_j\}_{j \geq j_0}$, of closed linear subspaces $V_j \subset H$ is called a *multiresolution* or *multiscale analysis*, if

$$V_{j_0} \subset V_{j_0+1} \subset \ldots \subset V_j \subset V_{j+1} \subset \ldots H \tag{5}$$

and $\cup_{j \geq j_0} V_j$ is complete in H.

The nestedness and the closedness of the multiresolution analysis implies the existence of the *complement spaces* W_j such that $V_{j+1} = V_j \oplus W_j$.

We now assume that V_j and W_j are spanned by sets of basis functions

$$\Phi_j := \{\phi_{j,k}, k \in \mathcal{I}_j\}, \quad \Psi_j := \{\psi_{j,k}, k \in \mathcal{J}_j\}, \tag{6}$$

where $\mathcal{I}_j$ and $\mathcal{J}_j$ are finite or at most countable index sets. We refer to $\phi_{j,k}$ as *scaling functions* and $\psi_{j,k}$ as *wavelets*. The multiscale basis and the wavelet basis of H are given by

$$\Psi_{j_0,s} = \Phi_{j_0} \cup \bigcup_{j=j_0}^{j_0+s-1} \Psi_j, \quad \Psi = \Phi_{j_0} \cup \bigcup_{j \geq j_0} \Psi_j. \tag{7}$$

The dual wavelet system $\tilde{\Psi}$ generates a dual multiresolution analysis $\tilde{\mathcal{V}}$ with a dual scaling basis $\tilde{\Phi}_{j_0}$.

Polynomial exactness of order $N \in \mathbb{N}$ for the primal scaling basis and of order $\tilde{N} \in \mathbb{N}$ for the dual scaling basis is another desired property of wavelet bases. It means that $\mathbb{P}_{N-1}(\Omega) \subset V_j$ and $\mathbb{P}_{\tilde{N}-1}(\Omega) \subset \tilde{V}_j$, $j \geq j_0$, where $\mathbb{P}_m(\Omega)$ is the space of all algebraic polynomials on Ω of degree less or equal to m. The polynomial exactness of order $\tilde{N}$ on the dual side is equivalent to $\tilde{N}$ vanishing wavelet moments on the primal side, i.e.

$$\int_{\Omega} P(x)\,\psi_\lambda(x)\,dx = 0, \quad \text{for any } P \in \mathbb{P}_{\tilde{N}-1},\ \psi_\lambda \in \bigcup_{j \geq j_0} \Psi_j. \tag{8}$$

3. Primal scaling basis

A primal scaling basis is the same as the basis constructed in [4, 16]. This basis is generated from functions ϕ and ϕ_b. Let ϕ be a cubic B-spline defined on knots $[0, 1, 2, 3, 4]$. It can be written explicitly as:

$$\phi(x) = \begin{cases} \frac{x^3}{6}, & x \in [0,1], \\ -\frac{x^3}{2} + 2x^2 - 2x + \frac{2}{3}, & x \in [1,2], \\ \frac{x^3}{2} - 4x^2 + 10x - \frac{22}{3}, & x \in [2,3], \\ -\frac{x^3}{6} + 2x^2 - 8x + \frac{32}{3}, & x \in [3,4], \\ 0, & \text{otherwise}, \end{cases} \tag{9}$$

Then this function satisfies a scaling equation [16] :

$$\phi(x) = \frac{\phi(2x)}{8} + \frac{\phi(2x-1)}{2} + \frac{3\phi(2x-2)}{4} + \frac{\phi(2x-3)}{2} + \frac{\phi(2x-4)}{8}. \tag{10}$$

The function ϕ_b is a cubic B-spline defined on knots $[0, 0, 1, 2, 3]$. It is given by:

$$\phi_b(x) = \begin{cases} -\frac{11x^3}{12} + \frac{3x^2}{2}, & x \in [0,1], \\ \frac{7x^3}{12} - 3x^2 + \frac{9x}{2} - \frac{3}{2}, & x \in [1,2], \\ -\frac{x^3}{6} + \frac{3x^2}{2} - \frac{9x}{2} + \frac{9}{2}, & x \in [2,3], \\ 0, & \text{otherwise}. \end{cases} \tag{11}$$

The function ϕ_b satisfies a scaling equation [16]:

$$\phi_b(x) = \frac{\phi_b(2x)}{4} + \frac{11\phi(2x)}{16} + \frac{\phi(2x-1)}{2} + \frac{\phi(2x-2)}{8}. \tag{12}$$

For $j \in \mathbb{N}$ and $x \in [0,1]$ we set

$$\begin{aligned} \phi_{j,k}(x) &= 2^{j/2}\phi(2^j x - k),\ k = 2, \ldots 2^j - 2, \\ \phi_{j,1}(x) &= 2^{j/2}\phi_b(2^j x), \quad \phi_{j,2^j-1}(x) = 2^{j/2}\phi_b(2^j(1-x)). \end{aligned} \tag{13}$$

The graphs of the functions $\phi_{j,k}$ on the coarsest level $j = 2$ are displayed in Figure 7.

We define a wavelet ψ as

$$\psi(x) = -\frac{1}{2}\phi(2x) + \phi(2x-1) - \frac{1}{2}\phi(2x-2). \tag{14}$$

Then $\operatorname{supp}\psi = [0,3]$ and ψ has two vanishing wavelet moments, i.e.

$$\int_{-\infty}^{\infty} x^k \psi(x)dx = 0, \quad k = 0, 1. \tag{15}$$

The same wavelet was used in the construction of a wavelet basis for the space $L^2(\mathbb{R})$ in [13]. The graph of ψ is shown in Figure 7.

We define a boundary wavelet ψ_b by:

$$\psi_b(x) = \phi_b(2x) + m\phi(2x) + n\phi(2x-1), \tag{16}$$

where m and n are real parameters. In applications, the length of the support and the number of vanishing wavelet moments play a role. We consider four choices of parameters m and n:

a) $m = 0$, $n = 0$
b) $m = -0.75$, $n = 0$
c) $m = -0.45$, $n = 0$
d) $m = -1.35$, $n = 0.6$

These choices are optimal in the following sense: a) defines a wavelet with the shortest possible support, b) defines a wavelet with the shortest possible support among the wavelets of the form (16) with the first vanishing moment, c) corresponds to the wavelet with the shortest possible support among the wavelets of the form (16) with the second vanishing wavelet moment. Wavelet corresponding to d) has two vanishing moments. It is summarized in the following lemma.

Lemma 1. *a) The function* $\psi_b(x) = \phi_b(2x)$ *satisfies* $\operatorname{supp}\psi_b = [0, 1.5]$.
b) The function $\psi_b(x) = \phi_b(2x) - 0.75\,\phi(2x)$ *satisfies* $\operatorname{supp}\psi_b = [0, 2]$ *and*

$$\int_{-\infty}^{\infty} \psi_b(x)dx = 0. \tag{17}$$

c) The function $\psi_b(x) = \phi_b(2x) - 0.45\,\phi(2x)$ *satisfies* $\operatorname{supp}\psi_b = [0, 2]$ *and*

$$\int_{-\infty}^{\infty} x\psi_b(x)dx = 0. \tag{18}$$

d) The function $\psi_b(x) = \phi_b(2x) - 1.35\,\phi(2x) + 0.6\,\phi(2x-1)$ *satisfies* $\operatorname{supp}\psi_b = [0, 2.5]$,

$$\int_{-\infty}^{\infty} \psi_b(x)dx = 0, \quad \text{and} \quad \int_{-\infty}^{\infty} x\psi_b(x)dx = 0. \tag{19}$$

Proof. The length of the support of the function ψ_b is derived from the lengths of the supports of functions $\phi_b(2x)$, $\phi(2x)$, and $\phi(2x-1)$. By (9) and (11) we have $\operatorname{supp}\phi_b(2x) = [0, 1.5]$, $\operatorname{supp}\phi(2x) = [0, 2]$, and $\operatorname{supp}\phi(2x-1) = [0.5, 2.5]$. Since the functions $\phi_b(2x)$, $\phi(2x)$ and $\phi(2x-1)$ are given in the closed form, the formulas (17), (18), and (19) can be verified easily. $\square$

Thus, we can choose boundary wavelet with two vanishing moments and larger support or boundary wavelets with shorter supports but only with one or zero vanishing moments. If $f \in H_0^2(0,1)$ and f is constant or linear at the interval $[0, \epsilon]$, then f have to be zero at $[0, \epsilon]$. The same holds for the interval $[1-\epsilon, 1]$. Hence $f \in H_0^2(0,1)$ can not be nonzero constant or linear near the boundary and therefore in some applications such as adaptive wavelet methods the vanishing moments does not play the significant role for boundary wavelets. The graphs of boundary wavelets ψ_b are displayed in Figure 7. All the following lemmas and theorems are valid for the wavelet basis Ψ including the boundary wavelet with parameters m and n given by a), b), c), or d).

For $j \in \mathbb{N}$ and $x \in [0, 1]$ we define

$$\begin{aligned} \psi_{j,k}(x) &= 2^{j/2}\psi(2^j x - k + 2), k = 2, ..., 2^j - 1, \\ \psi_{j,1}(x) &= 2^{j/2}\psi_b(2^j x), \quad \psi_{j,2^j}(x) = 2^{j/2}\psi_b(2^j(1-x)). \end{aligned} \tag{20}$$

We denote

$$\begin{aligned} \Phi_j &= \left\{ \phi_{j,k} / \left| \phi_{j,k} \right|_{H_0^2(0,1)}, k = 1, \ldots, 2^j - 1 \right\}, \\ \Psi_j &= \left\{ \psi_{j,k} / \left| \psi_{j,k} \right|_{H_0^2(0,1)}, k = 1, \ldots, 2^j \right\}. \end{aligned} \tag{21}$$

Then the sets

$$\Psi^s = \Phi_2 \cup \bigcup_{j=2}^{1+s} \Psi_j \quad \text{and} \quad \Psi = \Phi_2 \cup \bigcup_{j=2}^{\infty} \Psi_j \tag{22}$$

are a multiscale wavelet basis and a wavelet basis of the space $H_0^2(0,1)$, respectively. We use $u \otimes v$ to denote the tensor product of functions u and v, i.e. $(u \otimes v)(x_1, x_2) = u(x_1)\, v(x_2)$. We set

$$\begin{aligned}
F_j &= \left\{ \phi_{j,k} \otimes \phi_{j,l} \,/\, |\phi_{j,k} \otimes \phi_{j,l}|_{H_0^2(\Omega)}, k, l = 1, \ldots, 2^j - 1 \right\} \\
G_j^1 &= \left\{ \phi_{j,k} \otimes \psi_{j,l} \,/\, |\phi_{j,k} \otimes \psi_{j,l}|_{H_0^2(\Omega)}, k = 1, \ldots, 2^j - 1, l = 1, \ldots 2^j \right\} \\
G_j^2 &= \left\{ \psi_{j,k} \otimes \phi_{j,l} \,/\, |\psi_{j,k} \otimes \phi_{j,l}|_{H_0^2(\Omega)}, k = 1, \ldots, 2^j, l = 1, \ldots 2^j - 1 \right\} \\
G_j^3 &= \left\{ \psi_{j,k} \otimes \psi_{j,l} \,/\, |\psi_{j,k} \otimes \psi_{j,l}|_{H_0^2(\Omega)}, k, l = 1, \ldots, 2^j \right\}
\end{aligned}$$

where $\Omega = (0,1)^2$. A wavelet basis and a multiscale wavelet basis of the space $H_0^2(\Omega)$ are defined as

$$\Psi_s^{2D} = F_2 \cup \bigcup_{j=2}^{1+s} \left(G_j^1 \cup G_j^2 \cup G_j^3 \right), \quad \Psi^{2D} = F_2 \cup \bigcup_{j=2}^{\infty} \left(G_j^1 \cup G_j^2 \cup G_j^3 \right). \tag{23}$$

Remark 1. Wavelet basis of the space $H^2(\Omega)$ can be constructed in a similar way. We add two boundary functions ϕ_{b1} and ϕ_{b2} that are B-splines on sequences of knots $[0,0,0,0,1]$ and $[0,0,0,1,2]$, respectively. Then scaling basis is generated from the functions ϕ_{b1}, ϕ_{b2}, ϕ_b and ϕ as in (13), see also [2], and boundary wavelets are constructed as appropriate linear combinations of ϕ_{b1}, ϕ_{b2} and ϕ_b in a similar way as above.

4. Refinement matrices

From the nestedness and the closedness of multiresolution spaces it follows that there exist *refinement matrices* $\mathbf{M}_{j,0}$ and $\mathbf{M}_{j,1}$ such that

$$\Phi_j = \mathbf{M}_{j,0}^T \Phi_{j+1}, \quad \Psi_j = \mathbf{M}_{j,1}^T \Phi_{j+1}. \tag{24}$$

In these formulas we view the sets of functions Φ_j and Ψ_j as column vectors with entries $\phi_{j,k}$, $k = 1, \ldots, 2^j - 1$, and $\psi_{j,k}$, $k = 1, \ldots, 2^j$, respectively.

Due to the length of the support of primal scaling functions, the refinement matrix $\mathbf{M}_{j,0}$ has the following structure:

$$\mathbf{M}_{j,0} = \begin{pmatrix} \mathbf{M}_L & & \\ & \mathbf{M}^I_{j,0} & \\ & & \mathbf{M}_R \end{pmatrix}. \tag{25}$$

where $\mathbf{M}^I_{j,0}$ is a $(2^{j+1}-3) \times (2^j - 3)$ matrix given by

$$\left(\mathbf{M}^I_{j,0}\right)_{m,n} = \begin{cases} \frac{h_{m+1-2n}}{\sqrt{2}}, & n = 1, \dots, 2^j - 3,\ 0 \le m+1-2n \le 4, \\ 0, & \text{otherwise}, \end{cases} \tag{26}$$

where

$$\mathbf{h} = [h_0, h_1, h_2, h_3, h_4] = \left[\frac{1}{8}, \frac{1}{2}, \frac{3}{4}, \frac{1}{2}, \frac{1}{8}\right] \tag{27}$$

is a vector of coefficients from scaling equation (10). We denote a vector of coefficients from scaling equation (12) by

$$\mathbf{h}_b = \left[h^b_0, h^b_1, h^b_2, h^b_3\right] = \left[\frac{1}{4}, \frac{11}{16}, \frac{1}{2}, \frac{1}{8}\right] \tag{28}$$

Then $\mathbf{M}_L = \frac{1}{\sqrt{2}} \mathbf{h}_b^T$ and the matrix $\mathbf{M}_R$ is obtained from a matrix $\mathbf{M}_L$ by reversing the ordering of rows.

It follows from the equations (14) and (16) that the matrix $\mathbf{M}_{j,1}$ is of the size $(2^{j+1}-1) \times 2^j$ and has the structure

$$\mathbf{M}_{j,1} = \frac{1}{\sqrt{2}} \begin{pmatrix} 1 & m & n & 0 & 0 & 0 & \dots & 0 \\ 0 & -\frac{1}{2} & 1 & -\frac{1}{2} & 0 & 0 & \dots & 0 \\ 0 & 0 & 0 & -\frac{1}{2} & 1 & -\frac{1}{2} & & 0 \\ \vdots & \vdots & & & & & & \vdots \\ 0 & \dots & 0 & 0 & -\frac{1}{2} & 1 & -\frac{1}{2} & 0 \\ 0 & \dots & 0 & 0 & 0 & n & m & 1 \end{pmatrix}^T \tag{29}$$

There also exist refinement matrices $\tilde{\mathbf{M}}_{j,0}$ and $\tilde{\mathbf{M}}_{j,1}$ corresponding to dual spaces that satisfy:

$$\tilde{\Phi}_j = \tilde{\mathbf{M}}^T_{j,0} \tilde{\Phi}_{j+1}, \quad \tilde{\Psi}_j = \tilde{\mathbf{M}}^T_{j,1} \tilde{\Phi}_{j+1}, \tag{30}$$

where the sets $\tilde{\Phi}_j$ and $\tilde{\Psi}_j$ are viewed as column vectors.

The Euclidean norm of a vector $\mathbf{v}$ is denoted by $\|\mathbf{v}\|_2$ and the spectral norm of the matrix $\mathbf{M}$ is denoted as $\|\mathbf{M}\|_2$. The following lemma is crucial for the proof of a Riesz basis property.

Lemma 2. *The norm of the matrix* $\tilde{\mathbf{M}}_{j,0}$ *satisfies* $\left\|\tilde{\mathbf{M}}_{j,0}\right\|_2 \leq 2^p, p = 1 + \frac{\ln 3}{\ln 4}$.

Proof. We prove the lemma for the choice c) of parameters for boundary wavelet, for choices a), b), and d) the proof is similar. We denote the entries of the matrix $\tilde{\mathbf{M}}_{j,0}$ as $\tilde{M}_{k,l}^{j,0}$, $k = 1, \ldots 2^{j+1} - 1$, $l = 1, \ldots, 2^j - 1$.

Due to biorthogonality of the sets $\Psi_j \cup \Phi_j$ and $\tilde{\Psi}_j \cup \tilde{\Phi}_j$ we have

$$\mathbf{M}_{j,0}^T \tilde{\mathbf{M}}_{j,0} = \mathbf{I}_j \tag{31}$$

and

$$\mathbf{M}_{j,1}^T \tilde{\mathbf{M}}_{j,0} = \mathbf{0}_j, \tag{32}$$

where $\mathbf{I}_j$ denotes the identity matrix and $\mathbf{0}_j$ denotes the zero matrix of the appropriate size.

From (29) and (32) we have

$$\tilde{M}_{1,l}^{j,0} = 0.45\, \tilde{M}_{2,l}^{j,0}, \quad \tilde{M}_{2^{j+1}-1,l}^{j,0} = 0.45\, \tilde{M}_{2^{j+1}-2,l}^{j,0}, \tag{33}$$

and

$$\tilde{M}_{k,l}^{j,0} = \frac{\tilde{M}_{k-1,l}^{j,0} + \tilde{M}_{k+1,l}^{j,0}}{2}, \quad \text{for } k \text{ odd}, \quad k = 3, \ldots, 2^{j+1} - 3. \tag{34}$$

We substitute these relations into (31) and we obtain a new system of equations $\mathbf{A}_j \mathbf{B}_j = \mathbf{I}_j$, where

$$\mathbf{A}_j = \frac{1}{\sqrt{2}} \begin{pmatrix} \frac{21}{20} & \frac{3}{8} & 0 & \ldots & & 0 \\ \frac{3}{8} & \frac{5}{4} & \frac{3}{8} & & & \vdots \\ 0 & \frac{3}{8} & \frac{5}{4} & \frac{3}{8} & & 0 \\ \vdots & & \ddots & \ddots & \ddots & \\ 0 & & & \frac{3}{8} & \frac{5}{4} & \frac{3}{8} \\ 0 & & \ldots & 0 & \frac{3}{8} & \frac{21}{20} \end{pmatrix} \tag{35}$$

and $\mathbf{B}_j$ contains $\tilde{M}_{k,l}^{j,0}$ for k even, i.e. the entries $B_{k,l}^j$ of the matrix $\mathbf{B}_j$ satisfy:

$$B_{k,l}^j = \tilde{M}_{2k,l}^{j,0}, \quad k, l = 1, \ldots 2^j - 1. \tag{36}$$

We factorize the matrix $\mathbf{A}_j$ as $\mathbf{A}_j = \mathbf{C}_j \mathbf{D}_j$, where

$$\mathbf{C}_j = \frac{1}{\sqrt{2}} \begin{pmatrix} \frac{9}{8} & \frac{3}{8} & 0 & 0 & \dots & 0 \\ \frac{3}{8} & \frac{5}{4} & \frac{3}{8} & & & \vdots \\ 0 & \frac{3}{8} & \frac{5}{4} & \frac{3}{8} & & 0 \\ \vdots & & \ddots & \ddots & \ddots & \\ 0 & & & \frac{3}{8} & \frac{5}{4} & \frac{3}{8} \\ 0 & \dots & 0 & 0 & \frac{3}{8} & \frac{9}{8} \end{pmatrix} \tag{37}$$

and

$$\mathbf{D}_j = \begin{pmatrix} \frac{37}{40} & 0 & 0 & \dots & 0 & 0 & \frac{1}{40(-3)^{2^j-3}} \\ \frac{1}{40} & 1 & 0 & & 0 & 0 & \frac{1}{40(-3)^{2^j-4}} \\ \frac{-1}{40\cdot 3} & 0 & 1 & & 0 & 0 & \frac{1}{40(-3)^{2^j-5}} \\ \vdots & \vdots & & \ddots & & \vdots & \vdots \\ \frac{1}{40(-3)^{2^j-5}} & 0 & 0 & & 1 & 0 & \frac{-1}{40\cdot 3} \\ \frac{1}{40(-3)^{2^j-4}} & 0 & 0 & & 0 & 1 & \frac{1}{40} \\ \frac{1}{40(-3)^{2^j-3}} & 0 & 0 & \dots & 0 & 0 & \frac{37}{40} \end{pmatrix}. \tag{38}$$

More precisely, the entries $D^j_{k,l}$ of the matrix $\mathbf{D}_j$ are given by:

$$\begin{aligned} D^j_{1,1} &= D^j_{2^j-1,2^j-1} = \frac{37}{40}, \\ D^j_{k,1} &= D^j_{2^j+1-k,2^j-1} = \frac{(-1)^k}{40\cdot 3^{k-2}}, \quad \text{for } k = 2, \dots, 2^j-1, \\ D^j_{k,k} &= 1, \quad \text{for } k = 2, \dots, 2^j-2, \\ D^j_{k,l} &= 0, \quad \text{otherwise.} \end{aligned} \tag{39}$$

It is easy to verify that $\tilde{\mathbf{C}}_j = \mathbf{C}_j^{-1}$ has entries:

$$\tilde{C}^j_{k,l} = \sqrt{2}\left(-\frac{1}{3}\right)^{|k-l|}, \tag{40}$$

and the matrix $\mathbf{D}_j^{-1}$ has the structure:

$$\mathbf{D}_j^{-1} = \begin{pmatrix} d_1^j & 0 & \dots & 0 & d_n^j \\ d_2^j & 1 & & 0 & d_{n-1}^j \\ \vdots & & \ddots & & \vdots \\ d_{n-1}^j & 0 & & 1 & d_2^j \\ d_n^j & 0 & \dots & 0 & d_1^j \end{pmatrix}, \tag{41}$$

with $n = 2^j - 1$ and

$$\begin{aligned} d_1^j &= \frac{40\,\alpha_n}{37},\ d_n^j = \frac{(-1)^{n-1}\,40\,\alpha_n}{37^2 \cdot 3^{n-2}}, \\ d_k^j &= (-1)^{k-1}\,\alpha_n \left(\frac{1}{37 \cdot 3^{k-2}} + \frac{3^k}{\beta_n}\right), \quad k = 2, \dots, n-1. \end{aligned} \tag{42}$$

where constants α_n and β_n are given by

$$\alpha_n = \left(1 - \frac{1}{37^2 \cdot 3^{2n-4}}\right)^{-1}, \quad \beta_n = 37^2 \cdot 3^{2n-3}. \tag{43}$$

Therefore $\mathbf{B}_j = \mathbf{A}_j^{-1} = \mathbf{D}_j^{-1}\mathbf{C}_j^{-1}$ and substituting it into (32) we obtain the entries of the matrix $\tilde{\mathbf{M}}_{j,0}$:

$$\tilde{M}_{2,l}^{j,0} = \frac{40\sqrt{2}\alpha_n}{37}\left(\frac{-1}{3}\right)^{|1-l|} + \frac{(-1)^{|n-1|}\,40\sqrt{2}\,\alpha_n}{37^2 \cdot 3^{n-2}}\left(\frac{-1}{3}\right)^{|n-l|}, \tag{44}$$

$$\tilde{M}_{2^{j+1}-2,l}^{j,0} = \tilde{M}_{2,2^j-l}^{j,0}, \tag{45}$$

and for $k \in (2, 2^{j+1} - 2)$ even:

$$\begin{aligned} \tilde{M}_{k,l}^{j,0} = \frac{\sqrt{2}}{(-3)^{|k-l|}} &+ \frac{\sqrt{2}\alpha_n\,(-1)^{k-1}}{(-3)^{|1-l|}}\left(\frac{1}{37 \cdot 3^{k-2}} + \frac{3^k}{\beta_n}\right) \\ &+ \frac{\sqrt{2}\alpha_n\,(-1)^{n-k}}{(-3)^{|n-l|}}\left(\frac{1}{37 \cdot 3^{n-k-1}} + \frac{3^{n+1-k}}{\beta_n}\right) \end{aligned} \tag{46}$$

The entries $\tilde{M}_{k,l}^{j,0}$ for k odd are given by (33) and (34).

It is well-known that for any matrix $\mathbf{M}$ of the size $m \times n$ with entries $M_{k,l}$:

$$\|\mathbf{M}\|_2 \le \sqrt{\|\mathbf{M}\|_1\,\|\mathbf{M}\|_\infty}, \tag{47}$$

where

$$\|\mathbf{M}\|_1 = \max_{l=1,\dots,n} \sum_{k=1}^{m} |M_{k,l}|\,, \quad \|\mathbf{M}\|_\infty = \max_{k=1,\dots,m} \sum_{l=1}^{n} |M_{k,l}|\,. \tag{48}$$

In our case, from (44), (48), and a formula for a sum of a geometric sequence we obtain:

$$\left\|\tilde{\mathbf{M}}_{j,0}\right\|_1 \le 3\sqrt{2} \quad \text{and} \quad \left\|\tilde{\mathbf{M}}_{j,0}\right\|_\infty \le 2\sqrt{2}. \tag{49}$$

Thus

$$\left\|\tilde{\mathbf{M}}_{j,0}\right\|_2 \le 2\sqrt{3} = 2^p \quad \text{for} \quad p = 1 + \frac{\ln 3}{\ln 4}. \tag{50}$$

□

The consequence of the proof of Lemma 2 is that the matrix $\mathbf{M}_j = (\mathbf{M}_{j,0}, \mathbf{M}_{j,1})$ representing the discrete wavelet transform is invertible.

Lemma 3. *The matrix* $\mathbf{M}_j = (\mathbf{M}_{j,0}, \mathbf{M}_{j,1})$ *is invertible.*

Proof. We prove the lemma for the choice c) of parameters for boundary wavelet, for other choices the proof is similar. The matrix $\mathbf{M}_j$ is invertible if and only if the matrix $\tilde{\mathbf{M}}_j = (\tilde{\mathbf{M}}_{j,0}, \tilde{\mathbf{M}}_{j,1})$ satisfying $\mathbf{M}_j^T \tilde{\mathbf{M}}_j = \mathbf{I}_j$ exists and is unique. The existence and uniqueness of the matrix $\tilde{\mathbf{M}}_{j,0}$ is already shown in the proof of Lemma 2. The entries $\tilde{M}_{k,l}^{j,1}$ of the matrix $\tilde{\mathbf{M}}_{j,1}$ satisfy for $l = 1, \dots, 2^{j+1}$:

$$\tilde{M}_{1,l}^{j,1} = \delta_{l,1} - 0.45\, \tilde{M}_{2,l}^{j,1}, \quad \tilde{M}_{2^{j+1}-1,l}^{j,1} = \delta_{l,1} - 0.45\, \tilde{M}_{2^{j+1}-2,l}^{j,1}, \tag{51}$$

and

$$\tilde{M}_{k,l}^{j,1} = \delta_{k,2l-1} + \frac{\tilde{M}_{k-1,l}^{j,1} + \tilde{M}_{k+1,l}^{j,1}}{2}, \; k \,\text{odd}, \; k = 3, \dots, 2^{j+1} - 3. \tag{52}$$

Using these relations we obtain a system of equations with the matrix $\mathbf{A}_j$ defined by (35). From the proof of Lemma 2 follows that $\mathbf{A}_j$ is invertible. Therefore the matrix $\tilde{\mathbf{M}}_{j,1}$ exists and is unique. □

5. Riesz basis on Sobolev spaces

For $j \geq 2$ we define a column vector

$$(\Gamma_j)_k = \begin{cases} \phi_{j,k}, & k = 1, 2, \ldots, 2^j - 1, \\ \psi_{j,k-2^j-1}, & k = 2^j, \ldots 2^{j+1} - 1. \end{cases} \tag{53}$$

The symbol $\langle \cdot, \cdot \rangle$ denotes the standard $L^2(\Omega)$ inner product. If $\mathbf{u}$ and $\mathbf{v}$ are two vectors of functions of the length n, then $\langle \mathbf{u}, \mathbf{v} \rangle$ denotes matrix with entries $\langle \mathbf{u}_k, \mathbf{v}_l \rangle$, $k, l = 1, \ldots, n$. We set $\mathbf{F}_j = \langle \Gamma_j, \Gamma_j \rangle$, where $\hat{\Gamma}_j = \mathbf{F}_j^{-1} \Gamma_j$. We denote

$$\mathcal{I}_j = \left\{1, 2, \ldots, 2^j - 1\right\} \quad \text{and} \quad \mathcal{J}_j = \left\{1, 2, \ldots, 2^j\right\} \tag{54}$$

and the entries of $\hat{\Gamma}_j$ as

$$\hat{\phi}_{j,k} = \left(\hat{\Gamma}_j\right)_k, k \in \mathcal{I}_j, \; \hat{\psi}_{j,k} = \left(\hat{\Gamma}_j\right)_{k+2^j-1}, k \in \mathcal{J}_j. \tag{55}$$

Since obviously

$$\left\langle \Gamma_j, \hat{\Gamma}_j \right\rangle = \mathbf{I}_j, \tag{56}$$

functions from $\hat{\Gamma}_j$ are duals to functions from Γ_j in the space V_{j+1}. Since $\mathbf{F}_j^{-1}$ is not a sparse matrix, these duals are not local. We define a projection P_j from V_{j+1} onto V_j by

$$P_j f = \sum_{k \in \mathcal{I}_j} \left\langle f, \hat{\phi}_{j,k} \right\rangle \phi_{j,k}. \tag{57}$$

Lemma 4. *Let* $f \in V_{j+1}$, $a_k^j = \left\langle f, \hat{\phi}_{j,k} \right\rangle$, $\mathbf{a}_j = \left\{a_k^j\right\}_{k \in \mathcal{I}_j}$, $j \geq 2$, *and* $\mathbf{S}_j : \mathbf{a}_{j+1} \mapsto \mathbf{a}_j$. *Then* $\|\mathbf{S}_j\|_2 \leq 2^p$, $p = 1 + \frac{\ln 3}{\ln 4}$.

Proof. We have

$$\begin{aligned} P_j f &= \sum_{k \in \mathcal{I}_j} a_k^j \phi_{j,k} = \sum_{k \in \mathcal{I}_j} \left\langle f, \hat{\phi}_{j,k} \right\rangle \phi_{j,k} \\ &= \sum_{k \in \mathcal{I}_j} \sum_{l \in \mathcal{I}_{j+1}} a_l^{j+1} \left\langle \phi_{j+1,l}, \hat{\phi}_{j,k} \right\rangle \phi_{j,k}. \end{aligned} \tag{58}$$

Therefore

$$a_k^j = \sum_{l \in \mathcal{I}_{j+1}} a_l^{j+1} \left\langle \phi_{j+1,l}, \hat{\phi}_{j,k} \right\rangle. \tag{59}$$

Let us denote

$$S_{l,k}^{j} = \left\langle \hat{\phi}_{j,k}, \phi_{j+1,l} \right\rangle, \quad \mathbf{S}_j = \left\{ S_{l,k}^{j} \right\}_{l \in \mathcal{I}_{j+1}, k \in \mathcal{I}_j} \tag{60}$$

then we can write $\mathbf{a}_j = \mathbf{S}_j \mathbf{a}_{j+1}$, and

$$\mathbf{S}_j = \left\langle \hat{\Phi}_j, \Phi_{j+1} \right\rangle = \left\langle \hat{\Phi}_j, \tilde{\mathbf{M}}_{j,0} \Phi_j + \tilde{\mathbf{M}}_{j,1} \Psi_j \right\rangle = \tilde{\mathbf{M}}_{j,0}. \tag{61}$$

By Lemma 2 the assertion is proved. □

Lemma 5. *A projection P_j satisfies*

$$\| P_m P_{m+1} \dots P_{n-1} \| \leq 2^{p\,(n-m)}, \quad p = 1 + \frac{\ln 3}{\ln 4}, \tag{62}$$

for all $2 \leq m < n$.

Proof. Let $f_n \in V_n$, $f_m = P_m P_{m+1} \dots P_{n-1} f_n$, $f_j = \sum_{k \in \mathcal{I}_j} a_k^j \phi_j$, $\mathbf{a}_j = \left\{ a_k^j \right\}_{k \in \mathcal{I}_j}$, $j = m, n$. It is known [2, 16] that $\{ \phi_{j,k}, k \in \mathcal{I}_j \}$ is a Riesz basis of $V_j = \operatorname{span} \Phi_j$ and there exist constants C_1 and C_2 independent of j such that:

$$C_1 \| \mathbf{a}_j \|_2 \leq \left\| \sum_{k \in \mathcal{I}_j} a_k^j \phi_j \right\| \leq C_2 \| \mathbf{a}_j \|_2 . \tag{63}$$

By Lemma 4 we have for $p = 1 + \frac{\ln 3}{\ln 4}$:

$$\begin{aligned} \| f_m \| &\leq C_2 \| \mathbf{a}_m \|_2 \leq C_2 \| \mathbf{S}_m \|_2 \| \mathbf{S}_{m+1} \|_2 \dots \| \mathbf{S}_{n-1} \|_2 \| \mathbf{a}_n \|_2 \\ &\leq C_2 2^{p(n-m)} \| \mathbf{a}_n \|_2 \leq \frac{C_2}{C_1} 2^{p(n-m)} \| f_n \| . \end{aligned} \tag{64}$$

Thus (62) is proved. □

Theorem 6. *The set Ψ is a Riesz basis of $H_0^2(0,1)$.*

Proof. By Lemma 5 and Theorem 5.3. from [16], the set

$$\left\{ 2^{-2} \phi_{j,k}, j \geq 2, k = 1, \dots 2^j \right\} \cup \left\{ 2^{-2j} \psi_{j,k}, j \geq 2, k = 1, \dots 2^j \right\} \tag{65}$$

is a Riesz basis of the space $H_0^{\mu}(0,1)$ for $1 + \frac{\ln \sqrt{3}}{\ln 2} < \mu < 2.5$.

Since obviously

$$c 2^{2j} \leq | \psi_{j,k} |_{H_0^2(\Omega)} \leq C 2^{2j}, \quad \text{for } j \geq 2, \quad k = 1, \dots, 2^j, \tag{66}$$

the set Ψ defined by (22) is a Riesz basis of the space $H_0^2(0,1)$. □

Theorem 7. *The set Ψ^{2D} is a Riesz basis of $H_0^2\left((0,1)^2\right)$.*

Proof. The theorem is a consequence of Lemma 6, (66), and Theorem 5.3. from [16]. □

6. Quantitative properties of constructed bases

In this section, we compare the condition numbers of the stiffness matrices for the biharmonic problem in two dimensions for different wavelet bases. For $\Omega = (0,1)^2$ we consider the biharmonic equation

$$\Delta^2 u = f \text{ on } \Omega, \quad u = \frac{\partial u}{\partial n} = 0 \text{ on } \partial\Omega, \tag{67}$$

where Δ is the Laplace operator and n is the outer unit normal vector. The variational formulation is $\mathbf{Au} = \mathbf{f}$, where $\mathbf{A} = \left\langle \Delta\Psi^{2D}, \Delta\Psi^{2D} \right\rangle$, $u = \mathbf{u}^T \Psi^{2D}$, and $\mathbf{f} = \left\langle f, \Psi^{2D} \right\rangle$. It is known that then $\operatorname{cond} \mathbf{A} \leq C < \infty$. Since $\mathbf{A}_s = \left\langle \Delta\Psi_s^{2D}, \Delta\Psi_s^{2D} \right\rangle$ is a part of the matrix $\mathbf{A}$ that is symmetric and positive definite, we have also $\operatorname{cond} \mathbf{A}_s \leq C$. The condition numbers of the stiffness matrices $\mathbf{A}_s$ are shown in Table 7.

A construction by Jia and Zhao from [16] is denoted as JZ11, a construction from [4] is denoted as CF12, a construction of multiwavelet basis from [22] is denoted as S09 and wavelet bases constructed in this paper are denoted as a), b), c), and d) according to the choice of parameters for the boundary wavelet. The size of the stifness matrix is $N \times N$ for wavelet bases constructed in this paper, it differs for other bases. The condition number for our wavelet bases is comparable to the wavelet basis from [16], but the difference is that wavelets from [16] have not vanishing moments and therefore can not be used in some applications such as adaptive wavelet methods. Wavelet bases from [4, 22] have significantly larger condition number.

Remark 2. We can also treat the fourth-order problem subject to nonhomogeneous Dirichlet boundary conditions:

$$\Delta^2 u = f \quad \text{on } \Omega, \quad u = g \text{ on } \partial\Omega, \quad \frac{\partial u}{\partial n} = h \text{ on } \partial\Omega. \tag{68}$$

Let $w \in H^2(\Omega)$ be a function such that

$$w = g \text{ on } \partial\Omega, \quad \frac{\partial w}{\partial n} = h \text{ on } \partial\Omega. \tag{69}$$

Then the solution u of the problem (68) can be computed as $u = w + \tilde{u}$, where $\tilde{u}$ solves the problem

$$\Delta^2 \tilde{u} = f - \Delta^2 w \text{ on } \Omega, \quad \tilde{u} = 0 \text{ on } \partial\Omega, \quad \frac{\partial \tilde{u}}{\partial n} = 0 \text{ on } \partial\Omega. \tag{70}$$

If $\Omega = (0,1)$, we can simply set w to be a Hermite cubic polynomial:

$$w(x) = Ax^3 + Bx^2 + Cx + D \tag{71}$$

with $A = 2g(0) - h(0) - 2g(1) + h(1)$, $B = -3g(0) + 2h(0) + 3g(1) - h(1)$, $C = -h(0)$, $D = g(0)$.

The case $\Omega = (0,1)^2$ can be treated in a similar way. Since in formulation (68), the values of normal derivative of u are not well defined at corners, we will consider more precise formulation:

$$\begin{aligned} w &= g \text{ on } \partial\Omega, \ \frac{\partial w}{\partial y}(x,0) = h_1(x), \ \frac{\partial w}{\partial x}(1,y) = h_2(y), \\ \frac{\partial w}{\partial y}(x,1) &= h_3(x), \ \frac{\partial w}{\partial x}(0,y) = h_4(y), \ x,y \in [0,1]. \end{aligned} \tag{72}$$

If $w \in C^2\left(\bar{\Omega}\right)$ then

$$\begin{aligned} h_1(0) &= \frac{\partial w}{\partial y}(0,0) = \frac{\partial g}{\partial y}(0,0), \\ \frac{\mathrm{d}h_1}{\mathrm{d}x}(0) &= \frac{\partial^2 w}{\partial x \partial y}(0,0) = \frac{\partial^2 w}{\partial y \partial x}(0,0) = \frac{\mathrm{d}h_4}{\mathrm{d}y}(0), \end{aligned} \tag{73}$$

and similarly at other corners. Therefore, we assume that

$$\begin{aligned} h_1(0) &= \frac{\partial g}{\partial y}(0,0), \ h_1(1) = \frac{\partial g}{\partial y}(1,0), h_3(0) = \frac{\partial g}{\partial y}(0,1), \\ h_3(1) &= \frac{\partial g}{\partial y}(1,1), \frac{\mathrm{d}h_1}{\mathrm{d}x}(0) = \frac{\mathrm{d}h_4}{\mathrm{d}y}(0), \ \frac{\mathrm{d}h_1}{\mathrm{d}x}(1) = \frac{\mathrm{d}h_2}{\mathrm{d}y}(0), \\ \frac{\mathrm{d}h_3}{\mathrm{d}x}(1) &= \frac{\mathrm{d}h_2}{\mathrm{d}y}(1), \ \frac{\mathrm{d}h_3}{\mathrm{d}x}(0) = \frac{\mathrm{d}h_4}{\mathrm{d}y}(1). \end{aligned} \tag{74}$$

We first construct a function u^1 that satisfies boundary conditions at the part of the boundary $\{[0,y], y \in [0,1]\} \cup \{[1,y], y \in [0,1]\}$. We set

$$u^1(x,y) = A(y)x^3 + B(y)x^2 + C(y)x + D(y) \tag{75}$$

with $A(y) = 2g(0,y) + h_4(y) - 2g(1,y) + h_2(y)$, $B(y) = -3g(0,y) - 2h_4(y) + 3g(1,y) - h_2(y)$, $C(y) = h_4(y)$, $D(y) = g(0,y)$. We define $\tilde{g} = g - u^1$ on $\partial\Omega$, $\tilde{h}_1(x) = h_i(x) - \frac{\partial u^1}{\partial y}(x,0)$ and $\tilde{h}_3(x) = h_3(x) - \frac{\partial u^1}{\partial y}(x,1)$. We construct a function u^2 that satisfies $u^2 = \tilde{g}$ on $\partial\Omega$ and

$$\frac{\partial u^2}{\partial y}(x,0) = \tilde{h}_1(x), \ \frac{\partial u^2}{\partial y}(x,1) = \tilde{h}_3(x), \ \frac{\partial u^2}{\partial x}(0,y) = \frac{\partial u^2}{\partial x}(1,y) = 0. \quad (76)$$

We set

$$u^2(x,y) = \tilde{A}(x)\, y^3 + \tilde{B}(x)\, y^2 + \tilde{C}(x)\, y + \tilde{D}(x) \quad (77)$$

with $\tilde{A}(x) = 2\tilde{g}(x,0) + \tilde{h}_1(x) - 2\tilde{g}(x,1) + \tilde{h}_3(x)$, $\tilde{B}(x) = -3\tilde{g}(x,0) - 2\tilde{h}_1(x) + 3\tilde{g}(x,1) - \tilde{h}_3(x)$, $\tilde{C}(x) = \tilde{h}_1(x)$, $\tilde{D}(x) = \tilde{g}(x,0)$. Due to (74) it can be simply verified that $w = u^1 + u^2$ satisfies (72).

7. Numerical example

In this section, we compare the quantitative behaviour of the adaptive wavelet method with a basis constructed in this paper and bases from [4, 22]. All these bases are formed by cubic splines. We first briefly review an adaptive wavelet method. The method was proposed by Cohen, Dahmen and DeVore in [8]. We use a slightly modified version from [3] with an adaptive matrix-vector multiplication from [5].

For $\Omega = (0,1)^2$ we consider the fourth-order problem (67). Let Ψ^{2D} be a wavelet basis constructed in this paper. As mentioned above, the original equation (67) can be reformulated as an equivalent biinfinite matrix equation $\mathbf{Au} = \mathbf{f}$, where $\mathbf{A} = \langle \Delta\Psi^{2D}, \Delta\Psi^{2D} \rangle$, $u = \mathbf{u}^T \Psi^{2D}$, and $\mathbf{f} = \langle f, \Psi^{2D} \rangle$. Thus the original problem is equivalent to the well-posed problem in l^2. While the classical adaptive methods uses refining and derefining a given mesh according to a-posteriori local error estimates, the wavelet approach is different. Instead of turning to a finite dimensional approximation, we try to devise a convergent iteration for the l^2-problem. Then all infinite-dimensional quantities have to be replaced by finitely supported ones and the routine for the application of the biinfinite-dimensional matrix $\mathbf{A}$ approximately have to be designed.

The simplest convergent iteration for the l^2-problem is a *Richardson iteration* which has the following form:

$$\mathbf{u}_0 := \mathbf{0}, \quad \mathbf{u}_{n+1} := \mathbf{u}_n + \omega(\mathbf{f} - \mathbf{A}\mathbf{u}_n), \quad n = 0, 1, \ldots. \quad (78)$$

For the convergence, the relaxation parameter ω has to satisfy

$$\rho := \|\mathbf{I} - \omega \mathbf{A}\|_2 < 1, \tag{79}$$

where $\|\cdot\|_2$ is a spectral norm. Then the iteration (78) convergences with an error reduction per step

$$\|\mathbf{u}_{n+1} - \mathbf{u}\|_2 \leq \rho \|\mathbf{u}_n - \mathbf{u}\|_2 , \tag{80}$$

where $\|\cdot\|_2$ is the Euclidean norm. Condition (79) is satisfied if $0 < \omega < \frac{2}{\lambda_{max}}$, where λ_{max} is the largest eigenvalue of $\mathbf{A}$. It is known that the optimal relaxation parameter $\hat{\omega}$ and the corresponding error reduction can be computed as

$$\hat{\omega} = \frac{2}{\lambda_{min} + \lambda_{max}}, \quad \rho(\hat{\omega}) = \frac{\lambda_{max} - \lambda_{min}}{\lambda_{max} + \lambda_{min}} = \frac{\kappa(\mathbf{A}) - 1}{\kappa(\mathbf{A}) + 1}. \tag{81}$$

where λ_{min} is the smallest eigenvalue of $\mathbf{A}$. Hence the estimate of the number of iterations needed to resolve the problem with desired accuracy depends on the condition number of the matrix $\mathbf{A}$ that can be estimated by $\mathbf{A}_{j_{max}}$, where j_{max} is the maximal level used in the computations.

In the algorithm the sparse representation of the vector $\mathbf{f}$ is needed. It can be found due to the relation:

$$\langle f, \psi_{j,k} \rangle \leq C 2^{-js} \left\| f \cdot \chi_{\operatorname{supp} \psi_{j,k}} \right\|_{H^s(\Omega)} , \tag{82}$$

where $f \in H^s(\operatorname{supp} \psi_{j,k}) \cap L^2(\Omega)$, $0 \leq s < d$, d is the number of vanishing moments of wavelet $\psi_{j,k}$, $\chi_{\operatorname{supp} \psi_{j,k}}$ is an indicator function and C is a constant independent of j. It ensures that in the regions where f is smooth the corresponding coefficients of $\mathbf{f}$ are very small and can be thresholded. For the proof see [23].

We provide a numerical example. We consider the equation (67) with a solution u given by

$$u(x, y) = v(x) v(y), \quad v(x) = x^2 \left(1 - e^{10x-10}\right)^2 . \tag{83}$$

The relation (82) is not guaranteed for boundary wavelets corresponding to a), b) and c). However, since there is only a small number of boundary wavelets in comparison to a number of all wavelets up to some maximal level j_{max}, the sparse representation of $\mathbf{f}$ can be constructed. The vector $\tilde{\mathbf{f}}^{j_{max}}$ that includes the entries of $\mathbf{f}$ up to the level j_{max} was computed and its entries in absolute value were sorted. They are displayed in Figure 7 for the cases a) and d). The graphs almost coincides. The graphs for choices b) and d) lay between the graphs for a) and d). Since the structure of $\widetilde{\mathbf{f}}^{j_{max}}$ is similar for all choices of parameters, the sparse representations that are obtained by thresholding the coefficients smaller than some threshold ϵ are similar for all choices of parameters and the choice d) does not give significantly better results even though boundary wavelets have two vanishing moments.

The solution exhibits a sharp gradient near the point $[1, 1]$. We solve the problem by the method designed in [9] with the approximate multiplication of the stiffness matrix with a vector proposed in [5]. We use wavelets up to the scale $|\lambda| \leq 10$. The convergence history is shown in Figure 7.

In our experiments, the convergence rate, i.e. the slope of the curve, is similar for all bases. Since the initial threshold depends on Riesz bounds of the wavelet basis Ψ, the initial approximations are different and the curves are not similar. Due to low condition number of the stiffness matrix, bases a), b), and c) are significantly better in the number of iterations needed to resolve the problem with desired accuracy. The number of basis functions in cases a), b), and c) was about 1200 for an error in L^∞-norm about 10^{-6}. The number of all basis functions for full grid, i.e. basis functions of the level ten or less, is about 10^6, therefore by using an adaptive method the significant compression was achieved. It can seem that the number of iterations is quite large, but one could take into account that in the beginning the iterations were done for much smaller vector and the size of the vector increases successively.

Acknowledgments: The authors have been supported by the project "Modern numerical methods" No. 5844/16 financed by Technical University in Liberec.

References

[1] D. Černá, V. Finěk, Optimized construction of biorthogonal spline-wavelets, in: T.E. Simos et al. (Eds.), ICNAAM 2008, AIP Conference Proceedings 1048, American Institute of Physics, New York, 2008, pp. 134–137.

[2] D. Černá, V. Finěk, Construction of optimally conditioned cubic spline wavelets on the interval, Adv. Comput. Math. 34 (2011), 219–252.

[3] D. Černá, V. Finěk, Adaptive wavelet method for fourth-order elliptic problems, in: T.E. Simos et al. (Eds.), ICNAAM 2011, AIP Conference

Proceedings 1389, American Institute of Physics, New York, 2011, pp. 1606-1609.

[4] D. Černá, V. Finěk, Cubic spline wavelets with complementary boundary conditions, Appl. Math. Comput. 219 (2012), 1853–1865.

[5] D. Černá, V. Finěk, Approximate multiplication in adaptive wavelet methods, Cent. Eur. J. Math. 11 (2013), 972–983.

[6] X.F. Chen, J.W. Xiang, Solving diffusion equation using wavelet method, Appl. Math. Comput. 217 (2011) 6426-6432.

[7] C.K. Chui, E. Quak, Wavelets on a bounded interval, in: Numerical Methods of Approximation Theory (Braess, D.; Schumaker, L.L., eds.), Birkhäuser, 1992, pp. 53–75.

[8] A. Cohen, W. Dahmen, R. DeVore, Adaptive wavelet schemes for elliptic operator equations - convergence rates, Math. Comput. 70 (2001) 27–75.

[9] A. Cohen, W. Dahmen, R. DeVore, Adaptive wavelet methods II - beyond the elliptic case, Found. Math. 2 (2002) 203–245.

[10] W. Dahmen, B. Han, R.Q. Jia, A. Kunoth, Biorthogonal multiwavelets on the interval: cubic Hermite splines, Constr. Approx. 16 (2000) 221–259.

[11] W. Dahmen, A. Kunoth, K. Urban, Biorthogonal spline wavelets on the interval - stability and moment conditions, Appl. Comp. Harm. Anal. 6 (1999) 132–196.

[12] T.J. Dijkema, R. Stevenson, A sparse Laplacian in tensor product wavelet coordinates, Numer. 115 (2010), pp. 433–449.

[13] B. Han, Z. Shen, Wavelets with short support, SIAM J. Math. Anal. 38 (2006) 530–556.

[14] R.Q. Jia, S.T. Liu, Wavelet bases of Hermite cubic splines on the interval, Adv. Comput. Math 25 (2006) 23–39.

[15] R.Q. Jia, Spline wavelets on the interval with homogeneous boundary conditions, Adv. Comput. Math 30 (2009) 177–200.

[16] R.Q. Jia, W. Zhao, Riesz bases of wavelets and applications to numerical solutions of elliptic equations, Math. Comput. 80 (2011) 1525–1556.

[17] A. Khademi, K. Maleknejad, Filter matrix based on interpolation wavelets for solving Fredholm integral equations, Commun. Nonlinear Sci. Numer. Simul. 16 (2011) 4197-4207.

[18] S.T. Liu, Y. Xu, Graded Galerkin methods for high-order convection diffusion problem, Numer. Methods Partial Differential Eq. 25 (2009) 1261-1282.

[19] K. Maleknejad, M.N. Sahlan, The method of moments for solution of second kind Fredholm integral equations based on B-spline wavelets, Int. J. Comput. Math. 87 (2010) 1602-1616.

[20] K. Maleknejad, M. Yousefi, Numerical solution of the integral equation of the second kind by using wavelet bases of Hermite cubic splines, Appl. Math. Comput. 183 (2006) 134-141.

[21] M. Primbs, New stable biorthogonal spline-wavelets on the interval, Result. Math. 57 (2010) 121–162.

[22] A. Schneider, Biorthogonal cubic Hermite spline multiwavelets on the interval with complementary boundary conditions, Result. Math. 53 (2009) 407–416.

[23] K. Urban, Wavelet methods for elliptic partial differential equations. Oxford University Press, Oxford, 2009.

List of Tables

List of Figures

Table 1:

s	N	a)	b)	c)	d)	JZ11	CF12	S09
1	49	14.6	13.6	8.5	50.7	34.0	128.1	484.4
2	225	21.4	18.1	14.3	72.3	34.9	141.3	583.4
3	961	23.7	20.2	17.5	84.4	35.1	212.0	626.9
4	3969	24.5	21.4	18.2	91.3	35.3	257.6	653.5
5	16129	24.8	22.2	18.4	95.3	35.5	281.2	673.2
6	65025	25.2	22.6	18.6	98.0	35.8	297.2	689.4

Figure 1.

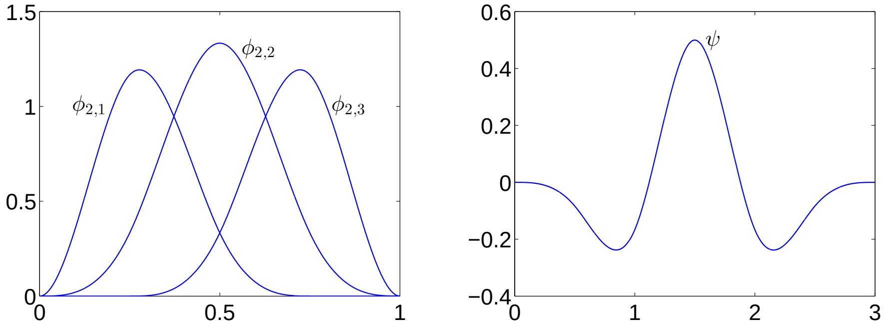

Figure 2.

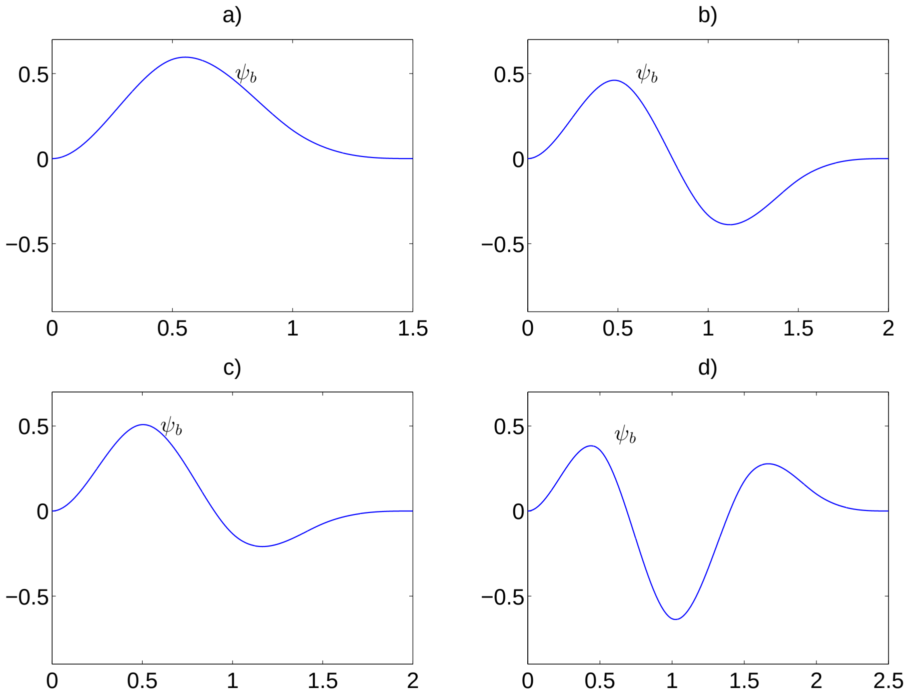

a)
ψ_b
0.5
0
−0.5
0
0.5
1
1.5
b)
ψ_b
0.5
0
−0.5
0
0.5
1
1.5
2
c)
ψ_b
0.5
0
−0.5
0
0.5
1
1.5
2
d)
ψ_b
0.5
0
−0.5
0
0.5
1
1.5
2
2.5

Figure 3.

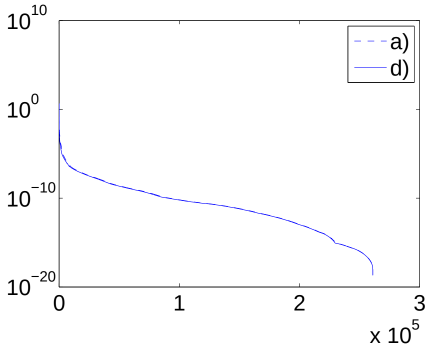

Figure 4.

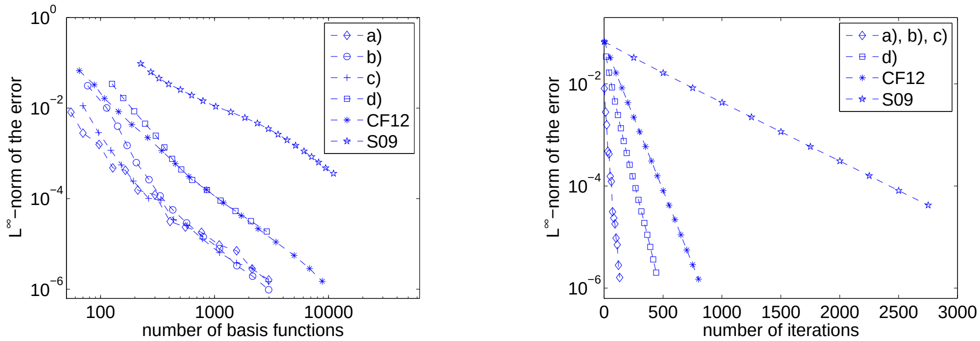

10^0
10^{-2}
10^{-4}
10^{-6}
L^∞–norm of the error
100
1000
10000
number of basis functions
a)
b)
c)
d)
CF12
S09
10^{-2}
10^{-4}
10^{-6}
L^∞–norm of the error
0
500
1000
1500
2000
2500
3000
number of iterations
a), b), c)
d)
CF12
S09